Heliyon 10 (2024) e28634

Contents lists available at ScienceDirect

Heliyon

journal homepage: www.cell.com/heliyon

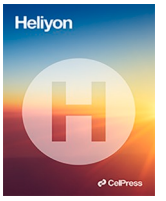

Research article

Synthesis, characterization, biological evaluation, and molecular docking studies of new 1,3,4-oxadiazole-thioether derivative as antioxidants and cytotoxic agents

Desta Gebretekle Shiferaw [a,b,*], Balakrishna Kalluraya [a]

[a] Department of Chemistry, Mangalore University, Karnataka, India
[b] Department of Chemistry, College of Natural and Computational Sciences, Aksum University, Tigray, Ethiopia

ARTICLE INFO

Keywords:
1,3,4-oxadiazole-thioether derivatives
Antioxidant activity
Cytotoxicity activity
Molecular docking

ABSTRACT

Oxadiazoles and their derivatives with thioether functionalities represent a new and exciting class of physiologically active heterocyclic compounds. Several molecules with these moieties play a vital role in pharmaceuticals because of their diverse biological activities. This paper describes a new class of 1,3,4- oxadiazole-2-thioethers with acetophenone, coumarin, and N-phenyl acetamide residues (S-alkylation), with the hope that the addition of various biologically active molecules will have a synergistic effect on anticancer activity. The structure of the synthesized title compounds was determined by the combined methods of IR, proton-NMR, carbon-13-NMR, and mass spectrometry. Furthermore, all the newly prepared molecules were assessed for their antioxidant activity. Furthermore, four compounds were assessed for their molecular docking interactions and cytotoxicity activity. The synthesized derivatives have shown moderate antioxidant activity compared to the standard BHA (butylated hydroxy anisole). The IC_{50} of the titled molecules (11b, 11c, 13b, and 14b) observed for in vitro anti-cancer activities were 11.20, 15.73, 59.61, and 27.66 g/ml at 72-h treatment time against the A549 cell lines, respectively. The tested compounds' biological evaluation showed that 11b is the most effective molecule in the series. In conclusion, the findings of this study suggest that the tested compounds, 1,3,4-oxadiazole-2-thioether derivative, have shown high cytotoxicity against human lung cancer diseases, which may serve for subsequent studies in the formulation of cancer-based drugs and future outlook for researchers.

1. Introduction

In recent years, compounds containing heteroatom nuclei have drawn much more attention because of their extensive chemotherapeutic activities. Oxadiazole, or furadiazole in the past, is the azole class of five-membered heteroaromatic compounds with one oxygen, two carbon, and two nitrogen atoms that exist in four different regioisomeric forms (Fig. 1) [1].

The 1,3,4-oxadiazole isomer typically displays lower lipophilicity (log D) than its isomeric partner [2]. The 1,2,3-oxadiazole ring is unstable and tautomerizes to a linear form of the diazo-ketone. 1,2,3-oxadiazole does not exist in its free form, but it can be found in rare mesoionic compounds known as sydnones [3].

* Corresponding author. Department of Chemistry, College of Natural and Computational Sciences, Aksum University, Tigray, Ethiopia.
E-mail address: destish2002@gmail.com (D.G. Shiferaw).

https://doi.org/10.1016/j.heliyon.2024.e28634
Received 12 December 2022; Received in revised form 20 March 2024; Accepted 21 March 2024
Available online 28 March 2024

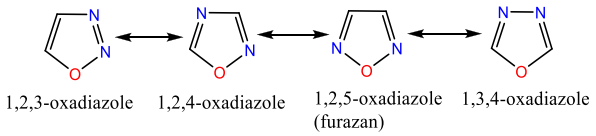

Fig. 1. Four isomeric forms of oxadiazoles.

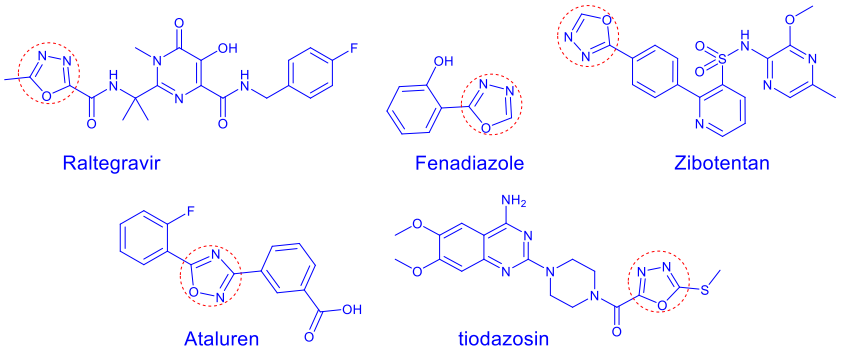

Fig. 2. Commercially available drugs having 1,3,4-oxadiazole moiety.

Furthermiles, the 1,3,4-oxadiazole nucleus has attracted the attention of synthetic organic and medicinal chemists as a bioisosteric replacement for carbonyl-containing compounds such as carboxylic acids, esters, and amides in the development of new drugs with anticancer activities [4]. There are different commercially available drugs that contain the 1,3,4-oxadiazole ring, such as the antiviral medication raltegravir [5], the hypnotic drug fenadiazole [6], the anticancer agent zibotentan [7], a medication for the treatment of Duchenne muscular dystrophy, ataluren [8], and an alpha-1 adrenergic receptor, tiodazosin [9]. As shown their structure in Fig. 2.

Furthermore, according to the reports in the literature, a 1,3,4-oxadiazole scaffold is well known for its antibacterial [10,11], antidiabetic [12], antimicrobial [13,14], anti-inflammatory [15], anticancer [16–18], antioxidant [19,20], and antiparasitic [21] activities. However, a minor structural change is happend in the 1,3,4-oxadiazole moiety, on the other hand, it could result in quantitative and qualitative biological activity. We attempted to synthesize new 1,3,4-oxadiazole ether derivatives incorporated into phenacyl, coumarin, and N-phenylacetamide moiety derivatives to improve antioxidant and anticancer drug activities while decreasing toxicity.

Docking is a method for predicting the preferred orientation of one molecule to another when a ligand and a target are bound together to form a stable complex [22]. The molecular docking method can model the interaction between a small molecule and a protein at the atomic level, characterizing small-molecule behavior in target protein binding sites and elucidating fundamental biochemical processes [23]. The docking process has two main steps: predicting the ligand conformation and its position and orientation within these sites (known as “pose”) and determining the binding affinity. The strength of association or binding affinity, between two molecules can be predicted using scoring functions. The study of a binding behavior is crucial for rational drug design and understanding basic biochemical processes [24,25].

2. Experimental

2.1. Materials and methods

The reagents and solvents used in the present work were obtained from Sigma-Aldrich Chemical Company Inc. And were used with further purification whenever needed. The melting points were measured using the open capillaries on an EQ 730 EQUIPTRONICS digital melting apparatus. Infrared spectra were recorded on KBr discs using a Shimadzu FT-IR 8000 spectrophotometer. ^{1}H NMR and ^{13}C NMR spectra were recorded on a JEOL 400 YH spectrometer (JNM-ECZ400S/LI) using DMSO-d_6 and $CDCl_3$ as solvents and TMS as a standard reference. All chemical shift values (ppm) are reported downfield from TMS, and the coupling constants (J) are reported in hertz (Hz). The following standardized abbreviations were used to indicate the splitting pattern (multiplicity): singlet (s), doublet (d), triplet (t), and multiplet (m). Mass spectra were recorded on a Shimadzu LC-MS-8030 mass spectrometer operating at 70 eV. Thin-layer chromatography was carried out using pre-coated silica gel plates (0.25 mm, 60G F254). A Vario-EL (Elementar-III) model analytical unit was used for the CHN analysis, and the values are ± 0.4% of the theoretical values. A spectrophotometer (model 106, systronics) and a multimode microplate reader (F1uoSTAR Omega, BMG Labtech, Germany) were used to measure the absorbance of antioxidants and cytotoxicity activities. 2,2-diphenyl-1-picrylhydrazyl (DPPH) and butylated hydroxyanisole (BHA) was purchased from SRKAY Chemicals and Equipment Center, India. Dulbecco’s Modified Eagle’s Medium (DMEM), fetal bovine serum (FBS), ethanol, dimethyl sulfoxide (DMSO), antibiotic-antimycotic solution, and 3-[4,5-dimethylthiazol-2-yl]-2,5-diphenyltetrazolium bromide (MTT) were purchased from Sigma-Aldrich. The human lung cancer (A549) cell was taken from Yenopeya Hospital, Mangalore, India.

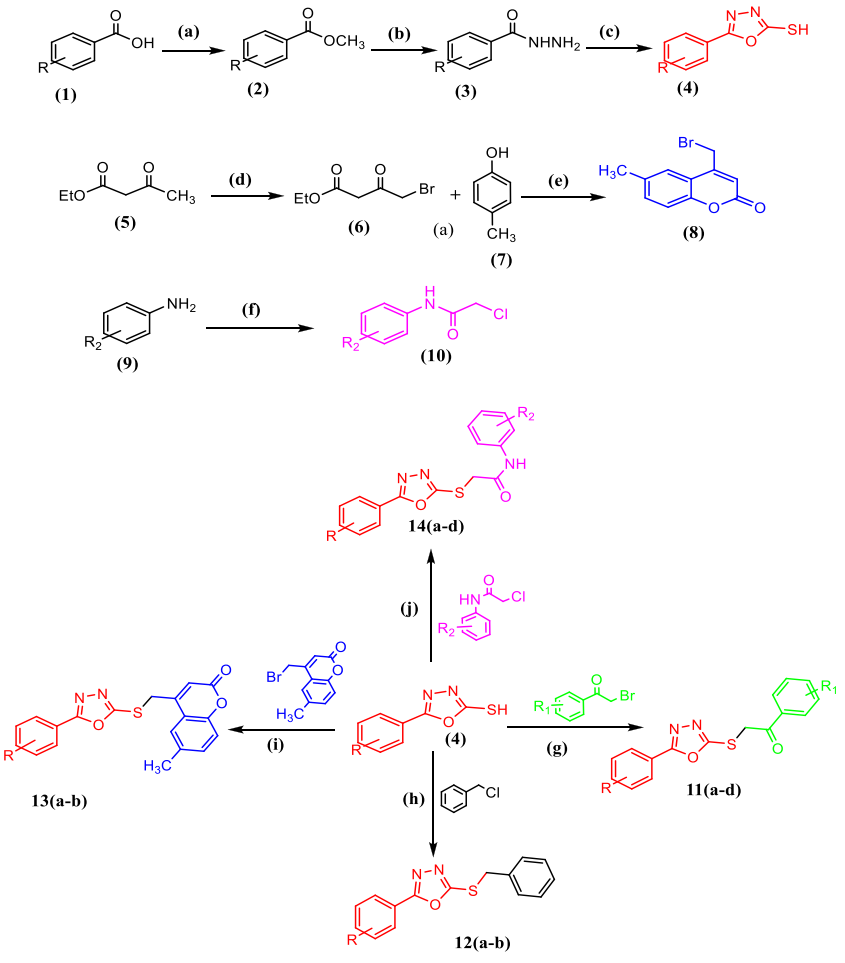

Scheme 1. Reagents and conditions: **(a)** MeOH, cat. H_2SO_4, 4 h reflux, (yield: 78–94%); **(b)** hydrazine hydrate, EtOH, 3 h reflux; **(c)** CS_2, KOH, EtOH, 4 h reflux; **(d)** Br_2, dry ether; 5 h stir, (yield: 65–80%); **(e)** conc. H_2SO_4, stir at 0 ^{0}C, then RT; **(f)** 2-chloroacetyl chloride, acetic acid, stir at RT; (g) Substituted phenacyl bromide, K_2CO_3, DMF, 4–6 h stir, (yield: 79–84%); **(h)** (chloromethyl)benzene, K_2CO_3, DMF, 4–6 h stir, (yield: 82–86%); **(i)** 4-(bromomethyl)-6-methyl-2H-chromen-2-one, K_2CO_3, DMF, 4–6 h stir, (yield: 76–80%); **(j)** substituted 2-chloro-N-phenylacetamide, K_2CO_3, DMF, 4–6 h stir, (yield: 77–87%).

2.2. Synthesis of the target compounds

The reaction sequences that lead to the synthesis of the final compound are depicted in Scheme 1. The 4-substituted methyl benzoate (2) was prepared using the standardized esterification method from its acid derivatives. 4-Substituted benzoyl hydrazine (3) was synthesized in good yield from the reaction of ester (2) with an excess of hydrazine hydrate in ethanol. Acid hydrazide (3) was intramolecularly cyclized with CS_2 to produce 5-(4-substituted phenyl)-1,3,4-oxadiazole-2-thiol (4). Compounds (4) were then successfully S-alkylated by reacting with appropriately substituted phenacyl bromide, benzyl chloride, 4-(bromomethyl)-6-methyl-2H-chromen-2-one, and 2-chloro-N-phenylacetamide to give compounds (1, 3, and 4-oxadiazole-2-thiol derivatives) (11, 12, 13, and 14) in good yields. This synthetic approach for constructing final compounds was achieved by a minor modification of the method reported in the literature [26]. The completion of the reaction was monitored by TLC using silica gel as the stationary phase and ethyl acetate-petroleum ether (8:2) as the mobile phase.

2.3. Reaction scheme of the starting materials and final products

.

2.4. Synthesis of S-substituted derivatives (11–14)

To a solution of 1,3,4-oxadiazole-thiols (**4**) (0.01 mmol) in dimethylformamide (25 ml), potassium carbonate (0.03 mmol) was

added gradually under ice-cooling. The reaction solution was stirred for 30 min, and then the appropriate phenacyl bromide, 4-methyl benzyl chloride, 4-(bromomethyl)-6-methyl-2H-chromen-2-one, or 2-chloro-N-phenylacetamide (0.01 mmol) was added portion-wise. The contents were stirred at room temperature for 4–6 h. Then, while constantly stirring, pour onto ice water. Filtration was used to collect the solid, which was then dried and recrystallized from DMF to yield the pure products 11(a-b), 12 (a-b), 13(a-d), and 14(a-d).

2.4.1. 2-((5-(4-Chlorophenyl)-1,3,4-oxadiazol-2-yl)thio)-1-(4-methoxyphenyl)ethan-1-one (11a)

Orange micro crystal, Yield 79%, m.p. 189–191 °C. IR ν_{max} (cm^{-1}): 1659 (C═O ketone); 1591 (C═N); 1508, 1466 (C═C); ^{1}H NMR (400 MHz, $CDCl_3$) δ: 3.89 (s, 3H, Ar-OCH_3), 4.94 (s,2H,-CH_2 –S), 6.99 (d, 2H, $J = 8.8$, Ar–H), 7.48 (d, 2H, $J = 8.8$, Ar–H),7.94 (d, 2H, $J = 8.4$, Ar–H), 8.04 (d, 2H, $J = 8.8$, Ar–H); ^{13}C NMR: 41.47, 55.59, 114.13, 121.95, 127.83, 127.94, 129.42, 130.94, 137.95, 164.26, 164.40, 165.08 and 190.44; MS (*m/z*): 363.00 ($M^+ + 2$); Anal. Calc, for $C_{17}H_{13}ClN_2O_3S$: C, 56.69; H, 3.64; N, 7.78. Found: C, 56.59; H, 3.63; N, 7.76.

2.4.2. 1-(4-Methoxyphenyl)-2-((5-(4-methoxyphenyl)-1,3,4-oxadiazol-2-yl)thio)ethan-1-one (11b)

Creamy needles, Yield 84%, m.p. 168–170 °C. IR ν_{max} (cm^{-1}): 1655(C═O), 1589 (C═N), 1503 (C═C); ^{1}H NMR (400 MHz, $CDCl_3$): δ: 3.84 (s, 3H, Ar-OCH_3), 3.87 (s, 3H, Ar-OCH_3), 5.10 (s, 2H,-CH_2 –S), 7.09 (d, 2H, $J = 7.08$ Hz, Ar–H), 7.12 (d, 2H, $J = 7.08$ Hz, Ar–H),7.86 (d, 2H, $J = 1.6$ Hz, Ar–H), 8.07 (d, 2H, $J = 1.56$ Hz, Ar–H); ^{13}C NMR: 41.47, 55.79, 114.12, 114.90, 115.01, 118.38, 127.73, 129.47, 160.54, 164.51, 165.40, 194.10; LC-MS (*m/z*): 357.00 ($M^+ + 1$); Anal. Calc. for $C_{18}H_{16}N_2O_4S$: C, 66.03; H, 4.51; N, 7.88. Found: C, 66.00; H, 4.53; N, 7.86.

2.4.3. 2-((5-(4-Chlorophenyl)-1,3,4-oxadiazol-2-yl)thio)-1-(p-tolyl)ethan-1-one (11c)

Golden yellow crystal, Yield 83%, m.p. 154–156 °C. IR ν_{max} (cm^{-1}): 1713 (C═O ketone), 1572 (C═N), 1504, 1472 (C═C); ^{1}H NMR (400 MHz, $CDCl_3$): δ: 2.43 (s, 3H, Ar-CH_3), 4.96 (s, 2H, –CH_2-S), 7.32 (d, 2H, $J = 8.0$ Hz, Ar–H), 7.47 (d, 2H, $J = 8.4$ Hz, Ar–H), 7.93 (d, 2H, $J = 8.2$ Hz, Ar–H), 7.95 (d, 2H, $J = 8.2$ Hz, Ar–H); ^{13}C NMR: 21.76, 41.62, 121.92, 127.92, 128.61, 129.40, 132.32, 137.93, 164.26, 145.40, 164.13, 165.07, 191.57; MS (*m/z*): 346.80 ($M^+ + 2$); Anal. Calc. for $C_{17}H_{13}ClN_2O_2S$: C, 6659.25; H, 3.81; N, 8.15. Found: C, 59.22; H, 3.80; N, 8.12.

2.4.4. 2-((5-(4-Methoxyphenyl)-1,3,4-oxadiazol-2-yl)thio)-1-(p-tolyl)ethan-1-one (11d)

Pale white micro crystal, yield 81%, m.p. 159–161 °C. IR ν_{max} (cm^{-1}): 1711 (C═O ketone), 1663, 1609, 1572 (C═N), 1501, 1474 (C═C); ^{1}H NMR (400 MHz, $CDCl_3$) δ: 2.43 (s, 3H, Ar-CH_3), 3.86 (s, 3H, Ar-OCH_3), 4.94 (s, 2H, –CH_2-S), 6.99 (d, 2H, $J = 8.8$ Hz, Ar–H), 7.32 (d, 2H, $J = 8.0$ Hz, Ar–H),7.93 (d, 2H, $J = 8.6$, Ar–H), 7.95 (d, 2H, $J = 8.4$ Hz, Ar–H); ^{13}C NMR: 21.76, 41.55, 55.42, 114.43, 115.99, 128.46, 128.63, 129.60, 132.40, 145.28, 162.26, 163.03, 165.87, 191.82; MS (*m/z*): 341.00 (M^+); Anal. Calc. for $C_{18}H_{16}N_2O_3S$: C, 63.55; H, 4.75; N, 8.26. Found: C, 63.51; H, 4.74; N, 8.23.

2.4.5. 2-(Benzylthio)-5-(4-chlorophenyl)-1,3,4-oxadiazole (12a)

Ash-colored needles yield 86%, m.p. 180–182 °C. IR ν_{max} (cm^{-1}): 1608 (C═N), 1501, 1474 (C═C); ^{1}H NMR (400 MHz, $CDCl_3$) δ:4.38 (s, 2H,-CH_2 –S), 7.16–7.40 (m, 5H, Ar–H), 7.23–7.60 (t, 1H, $J = 7.7$, 1.5 Hz, Ar–H), 7.31 (d, 2H, $J = 7.8$ Hz, Ar–H), 7.78 (d, 2H, $J = 8.2$ Hz), Ar–H), 7.96 (d, 2H, $J = 8.2$ Hz, Ar–H). ^{13}C NMR: 39.38, 124.20, 127.20, 127.80, 127.80, 128.70, 128.70, 128.90, 129.90, 129.40, 129.40, 134.40, 134.72, 164.89; MS (*m/z*): 304.20 (M^++2); Anal. Calc. for $C_{15}H_{11}ClN_2OS$: C, 59.58; H, 3.67; N, 9.29. Found: C, 59.50; H, 3.66; N, 7.89.25.

2.4.6. 2-(Benzylthio)-5-(4-methoxyphenyl)-1,3,4-oxadiazole (12b)

White needles yield 82%, m.p. 175–177 °C. IR ν_{max} (cm^{-1}): 1601 (C═N), 1501 (C═C); ^{1}H NMR (400 MHz, $CDCl_3$) δ: 3.88 (s, 3H, –OCH_3), 4.22 (s, 2H,-CH_2 –S), 7.19 (d, 2H, $J = 7.7$ Hz, Ar–H), 7.23 (t, 1H, $J = 7.7$, 1.5 Hz, Ar–H), 7.29 (d, 2H, $J = 8.8$ Hz, Ar–H), 7.39 (d, 2H, $J = 7.8$ Hz Ar–H), 7.87 (d, 2H, $J = 8.7$ Hz, Ar–H); ^{13}C NMR: 38.47, 55.59, 114.83,114.83, 115.92, 115.82, 118.45, 127.40, 127.80, 127.80, 128.82, 137.95, 160.62, 164.65; MS (*m/z*): 298.80 (M^+); Anal. Calc. for $C_{16}H_{14}N_2O_2S$: C, 68.45; H, 5.00; N, 9.92. Found: C, 68.40; H, 5.13; N, 9.89.

2.4.7. 4-(((5-(4-Chlorophenyl)-1,3,4-oxadiazol-2-yl)thio)methyl)-6-methyl-2H-chromen-2-one (13a)

Cream-colored crystals yield 80%, m.p. 178–180 °C. IR ν_{max} (cm^{-1}): 1713(C═O ketone); 1609 (C═N); 1504, 1475 (C═C); ^{1}H NMR (400 MHz, $CDCl_3$): 2.51 (s, 3H, Ar-CH_3), 3.52 (s,2H,-CH_2 –S), 6.99 (s, 1H, Ar–H),7.48–7.92 (m, 3H, Ar–H), 7.94 (d, 2H, $J = 8.4$ Hz, Ar–H), 8.04 (d, 2H, $J = 8.8$ Hz, Ar–H)); ^{13}C NMR: MS: 21.47, 44.1, 112.50,116.90, 120.94, 124.22, 127.00, 128.92, 129.35,132.24, 134.66, 135.46, 151.55,155.59, 161.55, 164.54; MS (*m/z*): 386.21 (M^++2); Anal. Calc. for $C_{19}H_{13}ClN_2O_3S$: C, 59.35; H, 3.40; N, 7.81. Found: C, 59.30; H, 3.41; N, 7.28.

2.4.8. 4-(((5-(4-Methoxyphenyl)-1,3,4-oxadiazol-2-yl)thio)methyl)-6-methyl-2H-chromen-2-one (13b)

Brownish micro-crystal yield 76%, m.p. 145–147 °C. IR ν_{max} (cm^{-1}): 1709 (C═O ketone), 1611 (C═N), 1503 1476 (C═C); ^{1}H NMR (400 MHz, $CDCl_3$) δ: 2.42 (s, 3H, Ar-CH_3), 3.86 (s,3H,-OCH_3), 4.61 (s, 2H, –CH_2 –S), 6.63 (s, 1H, Ar–H), 6.99–7.44 (m, 3H, Ar–H), 7.85 (d, 2H, $J = 8.8$ Hz, Ar–H), 7.92 (d, 2H, $J = 8.8$ Hz, Ar–H)); ^{13}C NMR: 21.04, 32.36, 55.46, 114.54, 115.68, 116.40, 117.30, 117.46, 123.79, 128.29, 133.33, 134.31, 148.57, 151.98, 160.32, 161.57, 162.47, 166.38; MS (*m/z*): 381.38 (M^++1); Anal. Calc. for $C_{20}H_{16}N_2O_4S$: C, 63.18; H, 4.23; N, 7.39. Found: C, 63.15; H, 4.24; N, 7.36.

2.4.9. N-(4-chlorophenyl)-2-((5-(4-chlorophenyl)-1,3,4-oxadiazol-2-yl)thio)acetamide (14a)

Dark brown crystal, yield 79%, m.p. 228–230 °C. IR ν_{max} (cm^{-1}): 3210 (N–H), 1710 (C═O), 1609 (C═N), 1501 (C═C);^{1}H NMR (400 MHz, $CDCl_3$): δ: 4.14 (s,2H, –CH_2-S), 7.24–7.27 (m, 2H, Ar–H), 7.58–7.62 (m, 2H, Ar–H), 7.63 (d, 2H, J = 8.4 Hz, Ar–H′), 7.88 (d, 2H, J = 7.2 Hz, Ar–H), 10.12 (s, 1H, NH); ^{13}C NMR: 38.66, 120.32, 120.64, 124.46, 128.92, 129.44, 129.62, 133.60, 134.59, 137.21, 165.24, 169.42; MS (*m/z*): 384.00 (M^+ + 4); Anal. Calc. for $C_{16}H_{11}Cl_2N_3O_2S$: C, 50.56; H, 2.91; N, 11.08. Found: C, 50.54; H, 2.92; N, 11.05.

2.4.10. 2-((5-(4-Chlorophenyl)-1,3,4-oxadiazol-2-yl)thio)-N-(4-nitrophenyl)acetamide (14b)

Yellow crystal, yield 87%, m.p. 238–240 °C. IR ν_{max} (cm^{-1}): 32101(N–H), 1709 (C═O amide), 1606 (C═N), 1494 (C═C); ^{1}H NMR (400 MHz, $CDCl_3$) δ: 4.22 (s,2H,–CH_2–S), 7.63 (d, 2H, J = 8.4 Hz, Ar–H), 7.82 (d, 2H, J = 7.2 Hz, Ar–H), 7.88 (d, 2H, J = 7.2 Hz, Ar–H), 8.17 (d, 2H, J = 7.2 Hz, Ar–H), 10.27 (s, 1H, NH); ^{13}C NMR: 38.56, 120.02, 124.44, 124.64, 128.94, 129.64, 134.65, 143.60, 144.69, 164.54, 169.46; MS (*m/z*): 392.00 (M^+ + 2); Anal. Calc. for $C_{16}H_{11}ClN_4O_4S$: C, 49.30; H, 2.83; N, 14.36. Found: C, 49.18; H, 2.84; N, 14.34.

2.4.11. N-(4-chlorophenyl)-2-((5-(4-methoxyphenyl)-1,3,4-oxadiazol-2-yl)thio)acetamide (14c)

Pale white crystal, yield 85%, m.p. 222–224 °C. IR ν_{max} (cm^{-1}): 3208 (N–H), 1709 (C═O amide), 1607 (C═N), 1497 (C═C); ^{1}H NMR (400 MHz, $CDCl_3$) δ: 3.82 (s, 3H, Ar-OCH_3), 4.22 (s, 2H, –CH_2-S), 7.08–7.21 (m, 3H, Ar– H), 7.59–7.64 (m, 1H, Ar–H), 7.83 (d, 2H, J = 8.0 Hz, Ar–H), 7.70 (d, 2H, J = 8.4 Hz, Ar–H), 10.21 (s, 1H, NH); ^{13}C NMR: 38.60, 55.82, 114.85, 115.92, 118.46, 120.42, 129.04, 133.65, 1136.66, 160.32, 164.44, 169.26; MS (*m/z*): 377.56 (M^+ + 2); Anal. Calc. for $C_{17}H_{14}ClN_3O_3S$: C, 54.42; H, 3.74; N, 11.23. Found: C, 54.33; H, 3.75; N, 11.18.

2.4.12. 2-((5-(4-Methoxyphenyl)-1,3,4-oxadiazol-2-yl)thio)-N-(4-nitrophenyl)acetamide (14d)

Yellow crystal, yield 77%, m.p. 204–206 °C.IR ν_{max} (cm^{-1}): 3229 (N–H), 1709 (C═O amide), 1608 (C═N), 1607 (C═C); ^{1}H NMR (400 MHz, $CDCl_3$) δ: 3.85 (s, 3H, Ar-OCH_3), 4.26 (s, 2H, –CH_2-S), 7.03 (d, 2H, J = 8.0 Hz, Ar–H), 7.82 (d, 2H, J = 8.4 Hz, Ar–H), 8.02 (d, 2H, J = 8.0 Hz, Ar–H), 8.17 (d, 2H, J = 8.4 Hz, Ar–H), 10.21 (s, 1H, NH); ^{13}C NMR: 38.61, 55.81, 114.81, 115.90, 118.42, 120.02, 124.20, 143.56,144.80, 160.65, 164.65, 168.86; MS (*m/z*): 387.11 (M^+ + 1); Anal. Calc. for $C_{17}H_{14}N_4O_5S$: C, 52.97; H, 3.64; N, 14.53. Found: C, 52.85; H, 3.65; N, 14.50.

2.5. Antioxidant study

The free radical scavenging activity of 1,3,4-oxadiazole-thioether derivatives was determined in vitro using the 2,2-diphenyl-1-picrylhydrazyl (DPPH) assay [27]. The test compounds were prepared with stock solutions (1 mg/ml) in DMSO and a 0.3 mM DPPH solution in ethanol. 150 μl and 200 μl of each sample was taken in three different test tubes and diluted up to 2.5 ml with ethanol so that the final concentrations were 60 and 80 μg/ml, respectively. The reaction mixture was vigorously mixed and allowed to stand for 30 min in the dark. The absorbance was measured at 518 nm using a Systronics spectrophotometer 106 apparatus. Butylated hydroxyanisole (BHA) was used as a control substance. The experiments were repeated three times, and the percentage of scavenging activity was calculated using the formula below.

$$\text{DPPH Scavenging Activity } (\%) = \frac{(\mathbf{Ac} - \mathbf{As})}{\text{Ac}}\mathbf{x}\ 100 \tag{1}$$

where Ac indicates the absorbance of the control reading and As shows the absorbance of the test samples. The means were used to express the results.

2.6. Cytotoxicity study

In the present study, among the synthesized compounds, four compounds (11b, 11c, 13b, and 14b) were tested for cytotoxicity activity in the MTT assay. Human A549 cells were grown in Dulbecco's Modified Eagle's Medium (DMEM) with 10% FBS and 1% antibiotic-antimycotic solution. Cells were kept at 37 °C and 5 % CO_2 in a humidified environment throughout the experiments.

The test chemicals' cytotoxicity were assessed using the Methyl thiazolyl Tetrazolium (MTT) assay. In 96-well Microtiter plates, cells were seeded at a density of 5000 cells per well. Following adherence, they were given various doses of the test chemical (solubilized in DMSO), viz., 6.25, 12.5, 25, 50, 100, and 200 μg/ml. After 24 and 72 h of treatment with test compounds, the MTT reagent was added to the wells and incubated at 37 °C for 4 h. Formazan crystals were produced and solubilized in DMSO before measuring absorbance at 570 nm with a multimode microplate reader (F1uoSTAR Omega, BMG Labtech). The percentage cytotoxicity of the test compound was calculated with respect to untreated cells [28].

$$\text{Percentage of inhibition } (\%) = \frac{\text{OD control} - \text{OD sample}}{\text{OD control}} * 100 \tag{2}$$

where: OD Control is the negative control absorbance. OD Sample is the absorbance of the test sample.

Table 1
DPPH scavenging activity of the final synthesized compounds at 60 and 80 μg/ml.

compounds	DPPH scavenging activity (% ± SD)		Compounds	DPPH scavenging activity (% ± SD)	
	At 60 μg/ml	At 80 μg/ml		At 60 μg/ml	At 80 μg/ml
11a	13.5 ± 0.25	13.0 ± 0.01	14a	19.4 ± 0.05	27.0 ± 0.04
11b	28.2 ± 0.15	24.6 ± 0.01	14b	18.9 ± 0.02	20.9 ± 0.00
11c	17.9 ± 0.05	20.9 ± 0.00	14c	19.5 ± 0.02	21.2 ± 0.00
11d	18.6 ± 0.00	21.1 ± 0.02	14d	19.6 ± 0.01	23.3 ± 0.00
12a	42.3 ± 0.12	34.7 ± 0.02	BHA	90.1 ± 0.00	89.2 ± 0.00
12b	22.3 ± 0.14	26.9 ± 0.08	Control	0	0
13a	21.5 ± 0.20	27.0 ± 0.06			
13b	38.7 ± 0.15	32.4 ± 0.03			

2.7. Molecular docking study

The docking studies of the compounds were carried out using the popular non-commercial Autodock 4.2/DAT. The target Protein Data Bank file was used to download the structure of Collapsin Response Mediator Protein 1 (PDB ID: CRMP1) (http://www.rcsb.org). Using the Pymol software, the macromolecule was prepared by removing molecules and all non-interacting ions. Once, it had been changed into an auto-docking macromolecule, it was used as a target macromolecule. The ligand structure was drawn in Chem 3D Pro, and their energy was minimized in open Babel. They were converted into auto dock ligand (pdbqt) files and then used for docking to the active site of the macromolecule. This conversion was carried out using Open Babel. All calculations are made in accordance with the docking's strict protein-fixed-ligand-flexible design. After docking, Discovery Studio 201957 was used to visualize the ligand-protein interactions. For additional docking studies, the method with an RMSD value of 2 A^0 was taken into consideration <2 A^0 was taken into consideration.

3. Results and discussion

3.1. Spectral results

The IR, ^{1}H NMR, ^{13}C NMR, and mass spectra data were used to characterize the novel final synthesized compounds. The procedures presented are easy, inexpensive, fast, environmentally benign, and provides good yields (76–87%). The results are described as follows:

The IR spectra of the S-alkylated products were recorded and interpreted [29]. The IR spectrum of 2-(5-(4-Chlorophenyl)-1,3,4-oxadiazol-2-yl)thio)-1-(4-methoxyphenyl)ethan-1-one (11a) showed characteristic absorption bands at 3040 and 2912 cm^{-1}, corresponding to aromatic and aliphatic C–H stretching vibrations, respectively. Furthermore, the absence of C═S absorption bands near 1384 cm^{-1} indicated that the product had been S-alkylated. Stretching C–S vibrations of 2-(5-(4-Chlorophenyl)-1,3,4-oxadiazol-2-yl)thio)-1-(4-methoxyphenyl)ethan-1-one (11a) were observed at 621 cm^{-1}. Similarly, the stretching band in the IR spectrum of N-(4-Chlorophenyl)-2-(5-(4-Chlorophenyl)-1,3,4-oxadiazol-2-yl)thio)acetamide (14a) was seen at 3210, 3046, and 2918 cm^{-1} due to (N–H), (aromatic C–H), and (aliphatic C–H), respectively. The stretching frequency of carbonyl (C═O) was observed at 710 cm^{-1}.

The ^{1}H NMR (400 MHz, $CDCl_3$) spectra of N-(4-chlorophenyl)-2-((5-(4-chlorophenyl)-1,3,4-oxadiazol-2-yl)thio)acetamide (14a) showed a singlet at δ 4.14 ppm for the S–CH_2 group, indicating the formation of an S-alkylated derivative. The aromatic protons of the two phenyl rings resonated as multiplets in the region of δ 7.24–7.88 ppm. In addition, a singlet appeared at δ 10.12 ppm correlated to the amide NH. Furthermore, the ^{13}C NMR spectrum manifested at δ 41.47 and 55.59 ppm due to S–CH_2 and OCH_3, respectively. The signals at δ 164.26 and 164.40 ppm appeared due to C-2 and C-5 carbon atoms in the 1,3,4-oxadiazole ring. The other peaks in the 114.13–137.95 ppm range were caused by the resonance of other aromatic carbon atoms. The characteristic peaks of C–S and C–O appeared at δ 165.24 and 169.42 ppm.

The 1,3,4-oxadiazole-2-thiol S-derivative structure was further confirmed by recording their mass spectra. In a typical example, the molecular ion peak of 2-((5-(4-Chlorophenyl)-1,3,4-oxadiazol-2-yl)thio)-1-(4-methoxyphenyl)ethan-1-one (11a) was observed at *m/z* 361, consistent with the chemical formula $C_{17}H_{13}ClN_2O_3S$. Similarly, the IR, ^{1}H NMR, ^{13}C NMR, and the remaining compounds' mass spectra are presented.

3.2. Antioxidant activity

The 2-diphenyl-1-picrylhydrazyl (DPPH) radical is a stable radical in organic solvents such as ethanol, methanol, and others. It appears to be purple and possesses a single unpaired electron. This radical can react with any molecule that emits a hydrogen atom or an electron, from purple to yellow. The discoloration degree indicates the samples' scavenging potential and hydrogen-donating ability. The antioxidant activity of the prepared compounds 11 (a-b), 12 (a-b), 13 (a-d), and 14 (a-d) was assessed using the DPPH free radical scavenging technique. The means were used to express the results. The data from the antioxidant activity experiments are tabulated in Table 1, and the bar diagram is depicted in Fig. 3.

Using the DPPH assay, the antioxidant activity results (Table 1 and Fig. 3) indicated that compounds 12a and 13b displayed

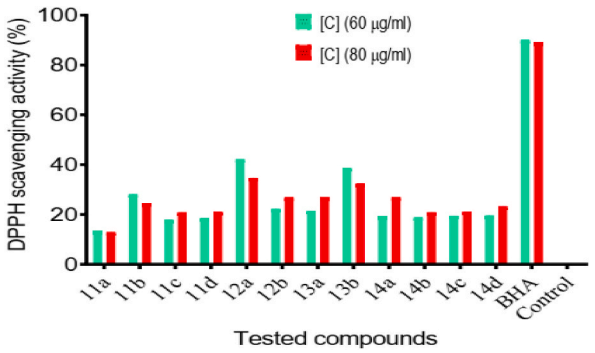

Fig. 3. Percentage of DPPH scavenging activity of the final synthesized compounds at 60 and 80 µg/ml.

Table 2
The percentage cytotoxicity of the tested compounds 11b, 11c, 13b, and 14b in 24 h.

Concentration	Tested compounds			
	11b	11c	13b	14b
	% Cytotoxicity (Mean % ± SD)	% Cytotoxicity (Mean % ± SD)	% Cytotoxicity (Mean % ± SD)	% Cytotoxicity (Mean % ± SD)
6.25	17.52 ± 7.68	10.73 ± 6.65	1.51 ± 0.89	7.21 ± 5.17
12.5	28.22 ± 3.69	13.99 ± 2.89	2.00 ± 0.89	15.31 ± 0.17
25	31.27 ± 6.57	21.71 ± 2.78	11.50 ± 2.67	35.86 ± 3.31
50	45.43 ± 2.77	23.58 ± 1.99	16.04 ± 1.200	53.75 ± 6.85
100	66.02 ± 3.29	44.73 ± 4.14	34.73 ± 2.89	63.32 ± 4.59
200	76.45 ± 2.84	76.91 ± 3.23	56.83 ± 5.87	74.47 ± 1.88

Table 3
The percentage Cytotoxicity of the tested compounds 11b, 11c, 13b, and 14b in 72 h.

Concentration	Tested compounds			
	11b	11c	13b	14b
	% Cytotoxicity (Mean % ± SD)	% Cytotoxicity (Mean % ± SD)	% Cytotoxicity (Mean % ± SD)	% Cytotoxicity (Mean % ± SD)
6.25	24.52 ± 0.42	17.31 ± 9.53	30.28 ± 19.98	50.98 ± 9.42
12.5	68.04 ± 4.303	60.87 ± 0.30	30.88 ± 4.19	55.62 ± 2.00
25	84.91 ± 6.24	68.86 ± 14.64	43.94 ± 5.04	69.12 ± 4.92
50	86.68 ± 2.43	71.18 ± 4.19	47.59 ± 8.86	81.05 ± 12.94
100	89.91 ± 1.51	84.92 ± 7.83	82.90 ± 8.86	88.31 ± 2.91
200	90.55 ± 0.79	91.45 ± 0.42	90.24 ± 0.24	89.17 ± 0.36

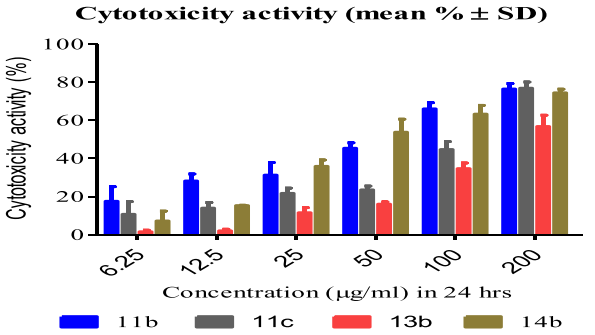

Fig. 4. Bar diagram comparing percentage cytotoxicity activity of the test compound **11b, 11c, 13b, and 14b** on A549 cells at 24 h..

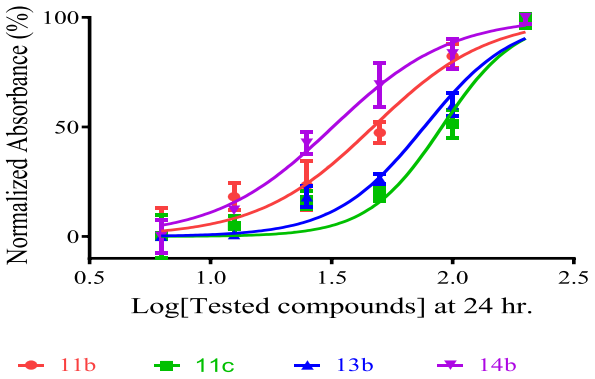

Fig. 5. The IC_{50} values of compounds 11b, 11c, 13b, and 14b in 24 h.

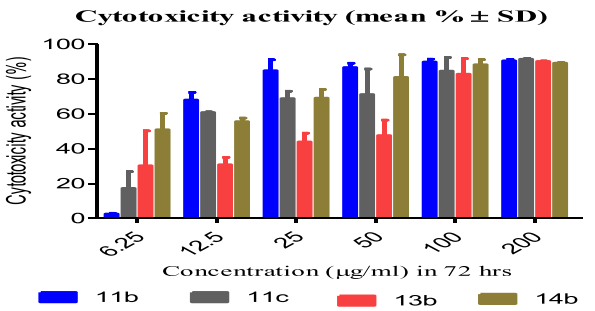

Fig. 6. Percentage cytotoxicity activity of the test compound 11b, 11c, 13b, and 14b on A549 cells 72 h.

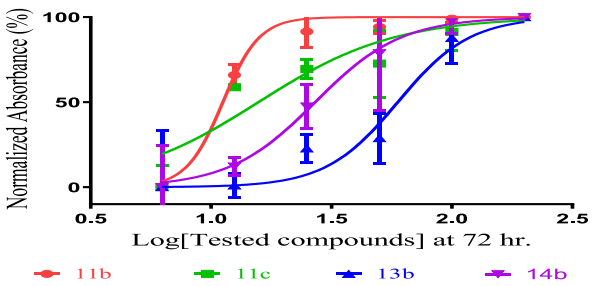

Fig. 7. The IC_{50} values of compounds 11b, 11c, 13b, and 14b in 72 h.

moderate scavenging activity at both concentrations, as compared to the standard BHA. Meanwhile, the scavenging activities of the remaining compounds exhibited poor antioxidant activity.

3.3. Cytotoxicity assay

In the present study, among the synthesized compounds, four compounds (11b, 11c, 13b, and 14b) were tested for cytotoxicity activity in the MTT assay. The human lung cancer (A549) cells were provided by the Yenapoya Research Center, Mangalore, Karnataka, India, and used for the study. The test method followed is based on the standard protocol [30]· Results were reported as percentage cytotoxicity and IC_{50} (half-maximal inhibitory concentration) values and indicated in Tables 2 and 3 and in Figs. 4–7.

log(inhibitor) vs. normalized response - Variable slope	Tested compounds, 24 h			
	11b	11c	13b	14b
$LogIC_{50}$ (µM)	1.671	1.956	1.883	1.505
IC_{50} (µM)	46.92	90.32	76.35	32.00
R^2	0.9439	0.9429	0.9538	0.9667

Table 4
Shows the binding affinity, number of Hydrogen bonds, and the amino acid involved in the interaction.

No.	Protein	Compound	Binding Affinity (Kcal/Mol)	No of the H bonds (drug-enzyme)	Amino acid is involved in the interaction
1	CMRP1	**11b**	−6.6	5	LYS (C:269), LYS (C:270), LYS (D:374), ASP (C:315), SER (D:319), TYR (D:316), LYS (A:258), LYS (D:258), ASP (D:262),GLU (D:229), LYS (B:270), SER (D:159)
2		**13b**	−8.2	1	ALA (B:265), ASP (B:262), LYS (A:269), LYS (A:270), BYR (B:316), LEU (C:266), LEU(A:266), ASP (C:262), SER (C:259)
3		**11c**	−7.2	1	LEU (B:266), LEU (D:266), ASP (B:262), ALA (B:265), LYS (A:269), LYS (B:269), LEU (A:266), ALA (A:265), ASP(A:262), LYS (C:270), LEU (C:266),
4		**14b**	−6.0	3	SER (A:259), LYS (C:270), ASP (A:262), LYS (C:269), TYR (D:316), THR (D:312), LYS(D:258), LYS (A:258, TYR (A:316),

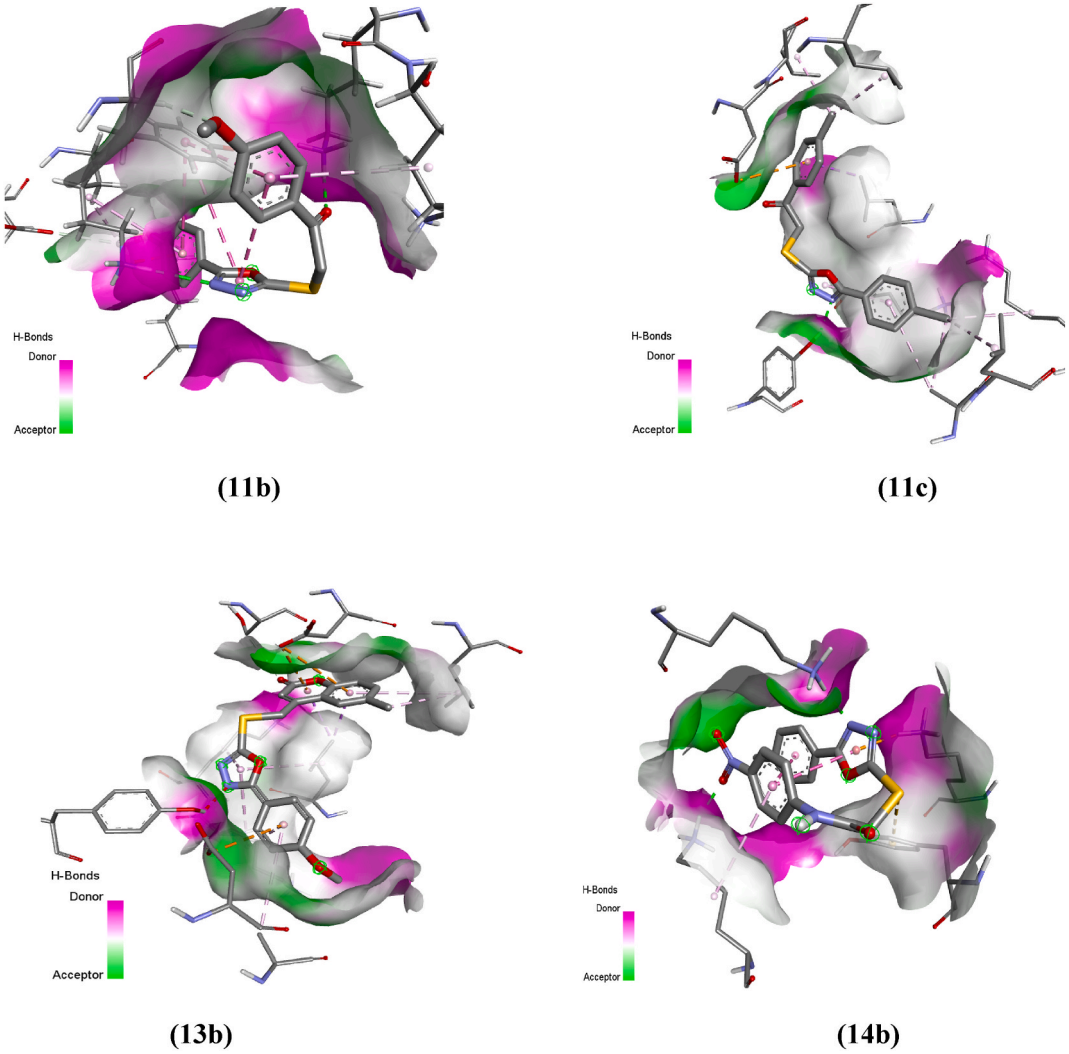

Fig. 8. 3D representation of the docking pose of the 11b, 11c, 13b, and 14b compounds showing hydrogen bond interactions.

log(inhibitor) vs. normalized response - Variable slope	Tested compounds at 72 h.			
	11b	11c	13b	14b
$LogIC_{50}$ (μM)	1.049	1.197	1.775	1.432
IC_{50} (μM)	11.20	15.73	59.61	27.06
R^2	0.9667	0.8149	0.8841	0.9003

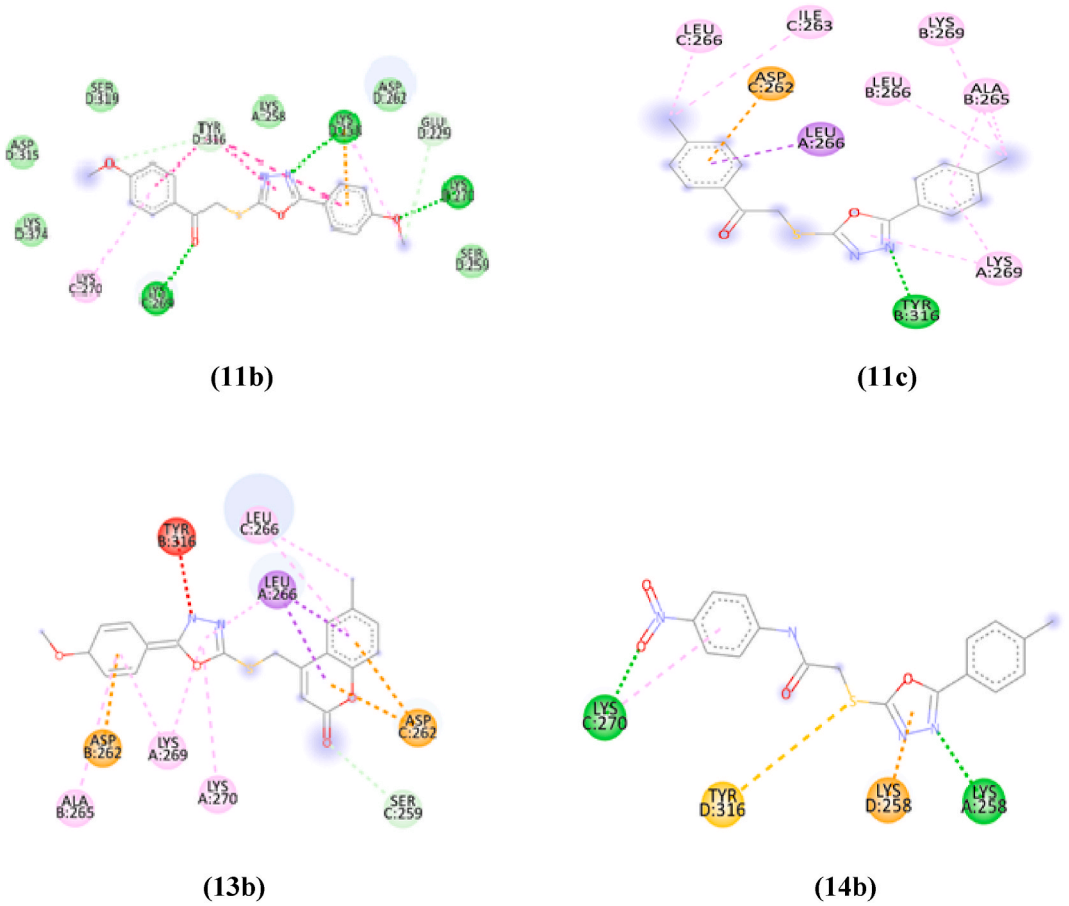

Fig. 9. 2D representation of the docking pose of the 11b, 11c, 13b, and 14b compounds.

The values are expressed as the mean standard deviation of triplicate measurements. All statistical analyses were performed using ANOVA and correlation in Microsoft Excel, and the graphs and IC_{50} values were drawn and calculated by GraphPad Prism 5 software. The comparison of the results was made according to cytotoxicity in vitro determination [31]; the preliminary screen uses:

The researchers discovered that the tested compounds had a significant dose and time-dependent cytotoxic effect on human lung cancer (A549) cells. Using this literature as a guide, the synthesized compounds (11b, 11c, 13b, and 14b) were evaluated for their in vitro cytotoxicity activity at a concentration of 6.25, 12.5, 25, 50, 100, and 200 μg/l. The results showed a significantly increased percent cytotoxicity of A549 cells in a dose- and time-dependent manner, according to the MTT assay results (Figs. 5 and 7). The IC_{50} value is the concentration of the tested drug required to kill 50% of the cells and can predict the degree of cytotoxicity. The data revealed that percent cytotoxicity increased with increasing concentration at both evaluation times (at 24 and 72 h). When the two evaluation times were compared, the tested compounds had significantly lower cytotoxic effects after 24 h than after 72 h. This indicates that a longer incubation period is necessary to see the effects of cytotoxicity on the cells that were weaker at a shorter incubation period. Among the tested compounds, 11b ($IC_{50} = 11.20$ M) and 11c ($IC_{50} = 15.73$ M) have shown the most active IC_{50} value at 200 μg/L in 72 h of treatment, whereas, the remaining compounds exhibited moderate cytotoxic activity.

3.4. Molecular docking studies

The promising cytotoxicity activities of the synthesized compounds inspired us to study their ability, to act as cytotoxicity agents in vitro. For this purpose, the four compounds were docked to the protein's active site (PDB ID: CMRP1), as explained in section 2.7 of this procedure. The results of the docking studies were represented in Table 4.

A molecular docking study was carried out on a few molecules to better understand the binding interactions of compounds at the active site of the protein. The docking studies in Table 4 showed that compounds 11b, 11c, 13b, and 14b have good binding interactions with the protein. The binding affinity ranges from −6.0 kcal/mol to −8.2 kcal/mol. By calculating the binding energy, hydrogen bond energy, and hydrophobic interactions with proteins, molecular docking studies forecast the biological activity of the newly synthesized compounds against both antioxidant and anticancer microbes. In vitro, compounds 13b and 11c also demonstrated promising anticancer activity. The docking poses of these compounds are shown in Figs. 8–10.

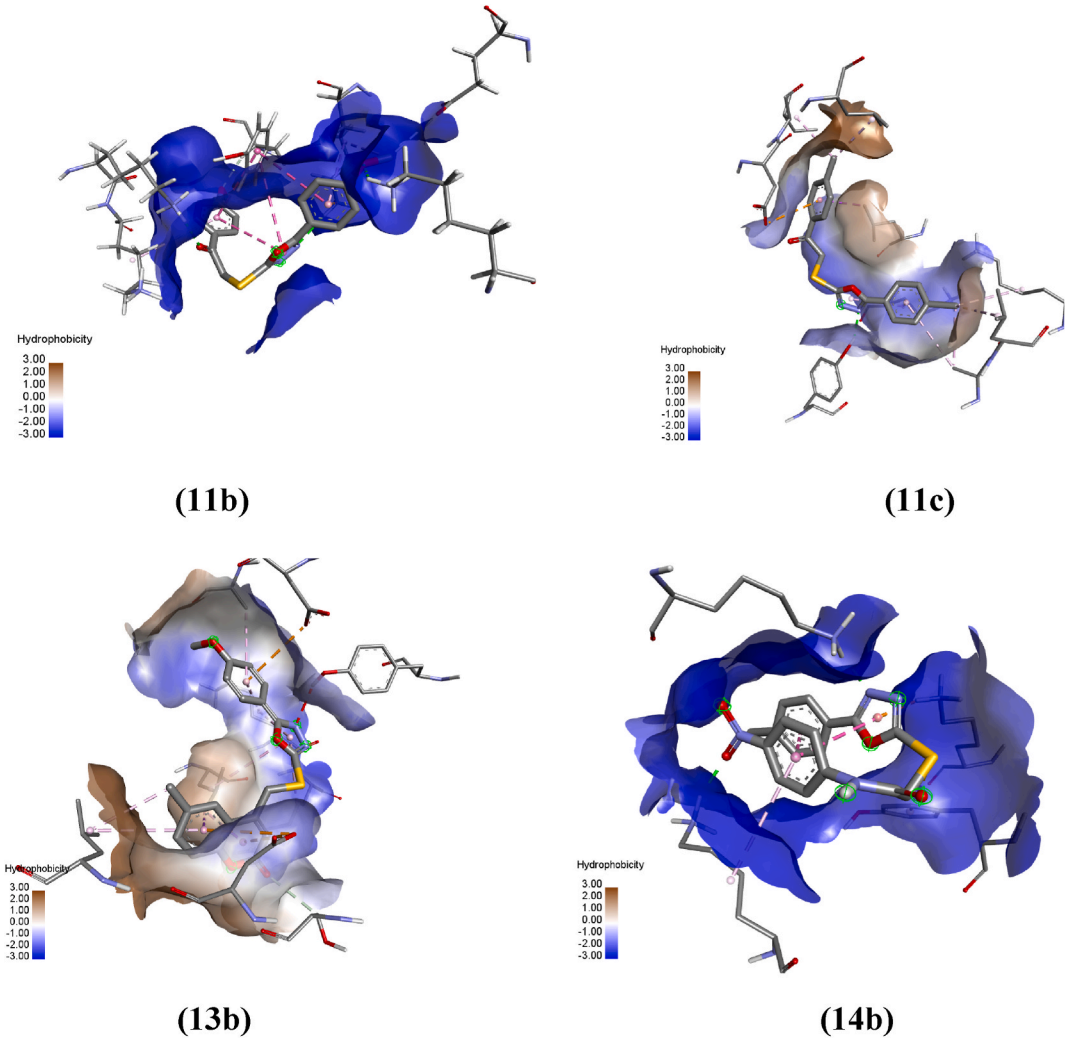

Fig. 10. 3D representation of the docking pose of the 11b, 11c, 13b, and 14b compounds showing hydrophilic interactions.

4. Conclusion

A series of 1,3,4-oxadiazole-2-thiol derivatives were designed and synthesized to discover new bioactive molecular frameworks with a broader range of pharmacological activities and good yields. Spectral and elemental analysis were used to characterize all the newly synthesized compounds. The compounds were tested for antioxidant and anticancer activity, as well as docking interactions. All of the synthesized compounds that were evaluated for their antioxidant activity showed poor to moderate actionable results. The four compounds screened for their anticancer activity exhibited moderate-to-good percentage cytotoxicity (cell death) against A549 cells at 24 and 72 h. Furthermore, the docking results agreed with in vitro studies, implying that these compounds could be further optimized and developed as lead compounds. Based on the findings, we can conclude that the synthesized series of compounds could be promising candidates for developing novel anticancer agents.

Funding statement

This research did not receive any specific grant from funding agencies in the public, commercial, or not-for-profit sectors.

Data availability statement

The characterization data for the synthesized compounds can be found at the supporting information.

CRediT authorship contribution statement

Desta Gebretekle Shiferaw: Writing – review & editing, Writing – original draft, Software, Methodology, Investigation, Formal analysis, Data curation, Conceptualization. **Balakrishna Kalluraya:** Visualization, Validation, Supervision, Formal analysis, Conceptualization.

Declaration of competing interest

The authors declare that they have no known competing financial interests or personal relationships that could have appeared to influence the work reported in this paper.

Acknowledgements

The authors express their gratitude to the Director, of Purse lab, Mangalore University, for providing the research facilities, and one of the authors, Desta, expresses appreciation to the Ethiopian Ministry of Education and Aksum University for financial support.

Appendix A. Supplementary data

Supplementary data to this article can be found online at https://doi.org/10.1016/j.heliyon.2024.e28634.

References

[1] A. Siwach, P.K. Verma, Therapeutic potential of oxadiazole or furadiazole containing compounds, BMC Chemistry 14 (2020) 70.
[2] J. Boström, A. Hogner, A. Llinas, E. Wellner, A.T. Plowright, Oxadiazoles in medicinal chemistry, J. Med. Chem. 55 (2012) 1817–1830.
[3] J. Joule, K. Mills, John Wiley & Sons, Hoboken, New Jersey, USA, 2010.
[4] A. SalahuddinMazumder, M.S. Yar, R. Mazumder, G.S. Chakraborthy, M.J. Ahsan, M.U. Rahman, Updates on the synthesis and biological activities of 1, 3, 4-oxadiazole: c review, Synth. Commun. 47 (2017) 1805–1847.
[5] C. Hicks, R.M. Gulick, Raltegravir: the first HIV type 1 integrase inhibitor, Clin. Infect. Dis. 48 (2009) 931–939.
[6] M.S.R. Murty, R. Penthala, L. R Nath, R. John Anto, Synthesis of salicylic acid-based 1, 3, 4-oxadiazole derivatives coupled with chiral oxazolidinones: novel hybrid heterocycles as antitumor agents, Lett. Drug Des. Discov. 11 (2014) 1133–1142.
[7] M.A. Esvelt, Z.T. Freeman, A.T. Pearson, J.R. Harkema, G.T. Clines, K.L. Clines, M.C. Dyson, M.J. Hoenerhoff, The endothelin-A receptor antagonist zibotentan induces damage to the nasal olfactory epithelium possibly mediated in part through type 2 innate lymphoid cells, Toxicol. Pathol. 47 (2019) 150–164.
[8] K. Bushby, R. Finkel, B. Wong, R. Barohn, C. Campbell, G.P. Comi, A.M. Connolly, J.W. Day, K.M. Flanigan, N. Goemans, K.J. Jones, Ataluren Treatment of Patients with Nonsense Mutation Dystrophinopathy, Muscle Nerve 50 (2014) 477–487.
[9] J. Chiang, G. Hermodsson, S. Oie, The effect of α1-acid glycoprotein on the pharmacological activity of α1-adrenergic antagonists in rabbit aortic strips, J. Pharm. Pharmacol. 43 (1991) 540–547.
[10] M. Arshad, 1, 3, 4-oxadiazole nucleus with versatile pharmacological applications: a review, Int. J. Pharma Sci. Res. 5 (2014) 1124.
[11] X. Song, P. Li, M. Li, A. Yang, L. Yu, L. Luo, D. Hu, B. Song, Synthesis and investigation of the antibacterial activity and action mechanism of 1, 3, 4-oxadiazole thioether derivatives, Pestic. Biochem. Physiol. 147 (2018) 11–19.
[12] R. Bhutani, D.P. Pathak, G. Kapoor, A. Husain, R. Kant, M.A. Iqbal, Anti-cancer and antimicrobial activity, in-silico ADME and docking studies of biphenyl pyrazoline derivatives, Bioorg. Chem. 77 (2018) 6–15.
[13] G.C. Ramaprasad, B. Kalluraya, B.S. Kumar, R.K. Hunnur, Synthesis and biological property of some novel 1, 3, 4-oxadiazoles, Eur. J. Med. Chem. 45 (2010) 4587–4593.
[14] B. Kalluraya, B. Lingappa, S.R. Nooji, Synthesis and biological study of some novel 4-[5-(4, 6-Disubstituted-2-thiomethylpyrimidyl)-4′-amino-1, 2, 4-triazol-3′-yl] thioacetyl-3-arylsydnones, Phosphorus Sulfur Silicon Relat. Elem. 182 (2007) 1393–1401.
[15] A. Husain, M. Ajmal, Synthesis of novel 1, 3, 4-oxadiazole derivatives and their biological properties, Acta Pharm. 59 (2009) 223–233.
[16] U. Çevik, B.N. Sağlık, D. Osmaniye, S. Levent, B. Kaya Çavuşoğlu, A.B. Karaduman, Ö. Atlı Eklioğlu, Y. Özkay, Z.A. Kaplancıklı, Synthesis, anticancer evaluation and molecular docking studies of new benzimidazole-1, 3, 4-oxadiazole derivatives as human topoisomerase types I poison, J. Enzym. Inhib. Med. Chem. 35 (2020) 1657–1673.
[17] M.M. Alam, A.S. Almalki, T. Neamatallah, N.M. Ali, A.M. Malebari, S. Nazreen, Synthesis of new 1, 3, 4-oxadiazole-incorporated 1, 2, 3-triazole moieties as potential anticancer agents targeting thymidylate synthase and their docking studies, Pharmaceuticals 13 (2020) 390.
[18] N. Polka, S. Malthum, J.S. Anireddy, U. Brahma, G.M. Naidu Vegi, Design, synthesis, and anticancer evaluation of new 1, 3, 4-oxadiazole thioether derivatives, Russ. Chem. Bull. 70 (2021) 580–584.
[19] E.A. Musad, R. Mohamed, B.A. Saeed, B.S. Vishwanath, K.L. Rai, Design, synthesis, and anticancer evaluation of new 1, 3, 4-oxadiazole thioether derivatives, Bioorg. Med. Chem. Lett 21 (2011) 3536–3540.
[20] M. Malhotra, R.K. Rawal, D. Malhotra, R. Dhingra, A. Deep, P.C. Sharma, Synthesis, characterization and pharmacological evaluation of (Z)-2-(5-(biphenyl-4-yl)-3-(1-(imino) ethyl)-2, 3-dihydro-1, 3, 4-oxadiazol-2-yl) phenol derivatives as potent antimicrobial and antioxidant agents, Arab. J. Chem. 1 (2017) 1022–1031.
[21] P. Pitasse-Santos, V. Sueth-Santiago, M.E. Lima, Antimicrobial activity and SAR of 2, 5-disubstituted 1, 3, 4-oxadiazole derivatives, J. Braz. Chem. Soc. 29 (2018) 435–456.
[22] T. Lengauer, M. Rarey, Computational methods for biomolecular docking, Curr. Opin. Struct. Biol. 6 (1996) 402–406.
[23] B.J. McConkey, V. Sobolev, M. Edelman, The performance of current methods in ligand–protein docking, Curr. Sci. 83 (2002) 845–855.
[24] D.B. Kitchen, H. Decornez, J.R. Furr, J. Bajorath, Docking and scoring in virtual screening for drug discovery: methods and applications, Nat. Rev. Drug Discov. 3 (2004) 935–949.
[25] T. Mostashari-Rad, R. Arian, H. Sadri, A. Mehridehnavi, M. Mokhtari, F. Ghasemi, A. Fassihi, Study of CXCR4 chemokine receptor inhibitors using QSPR and molecular docking methodologies, J. Theor. Comput. Chem. 18 (2019) 1950018.
[26] B. Mochona, E. Mazzio, M. Gangapurum, N. Mateeva, K. Redda, Synthesis of some benzimidazole derivatives bearing 1, 3, 4-oxadiazole moiety as anticancer agents, Chem. Sci. Trans. 4 (2015) 534.
[27] L.L. Mensor, F.S. Menezes, G.G. Leitão, A.S. Reis, T.C. Santos, C.S. Coube, S.G. Leitão, Screening of Brazilian plant extracts for antioxidant activity by the use of DPPH free radical method, Phytother Res. 15 (2001) 127–130.

[28] T. Mosmann, Rapid colorimetric assay for cellular growth and survival: application to proliferation and cytotoxicity assays, J. Immunol. Methods 65 (1983) 55–63.
[29] S.B. Nimse, D. Pal, Free radicals, natural antioxidants, and their reaction mechanisms, RSC Adv. 5 (2015) 27986–28006.
[30] J.D. Chencharick, K.L. Mossman, Nutritional consequences of the radiotherapy of head and neck cancer, Cancer 51 (1983) 811–815.
[31] P. Wiji Prasetyaningrum, A. Bahtiar, H. Hayun, Synthesis and cytotoxicity evaluation of novel asymmetrical mono-carbonyl analogs of curcumin (AMACs) against Vero, HeLa, and MCF7 Cell Lines, Sci. Pharm. 86 (2018) 25.